

Scattering plane waves by a dielectric cylinder with periodically modulated permittivity at oblique incidence

Evgeny N. Bulgakov^{1,2} and Almas F. Sadreev¹

¹*Kirensky Institute of Physics, Federal Research Center KSC SB RAS, 660036 Krasnoyarsk, Russia*

²*Siberian State Aerospace University, Krasnoyarsk 660014, Russia*



(Received 20 February 2018; published 28 June 2018)

For scattering of electromagnetic waves by a dielectric cylinder with periodically modulated permittivity we focus on the vicinity of the frequency of the wave with regard to the eigenfrequencies of bound states in the continuum. Then response of the cylinder becomes extremely sensitive to the angle of incidence and polarization of the plane wave. The cross section of the scattering of electromagnetic waves with mixed polarization undergoes crucial change from the Bragg shape to the Fano shape by rotation of the polarization that paves a way to tuning of Fano resonances by an external source.

DOI: [10.1103/PhysRevA.97.063856](https://doi.org/10.1103/PhysRevA.97.063856)

I. INTRODUCTION

The problem of diffraction of a plane wave by a homogeneous dielectric cylinder was solved 100 years ago by Rayleigh [1] at normal incidence and by Wait at oblique incidence [2]. In this paper we consider the scattering of a plane wave by the inhomogeneous dielectric cylinder at oblique incidence. For the case of periodic modulation of the permittivity along the cylinder axis $\epsilon(z) = \epsilon(z + h)$ (see Fig. 1) it was shown recently that such a cylinder supports bound states in the radiation continuum (BICs) [3,4]. They have discrete eigenfrequencies above the light line, i.e., infinite Q factor. Therefore their response onto the incident wave can be enormously large in a vicinity of the eigenfrequency of the BIC [5–9] accompanied by the collapse of the Fano resonance that is a generic feature of the scattering inherent to BICs [10–12].

In the present paper we focus on the excitation of BIC modes with orbital angular momentum by plane waves as dependent on angle of incidence. Such BICs were found in a previous paper [3]. Moreover we consider the case of a plane wave with mixed polarization and show that the cross section of scattering undergoes crucial changes from the Bragg shape to the Fano shape for variation of the polarization. This result opens a way of tuning of Fano resonances by an external source not addressing tuning of material parameters [13]. This effect becomes especially sensitive to variation of external parameters in the vicinity of the BIC frequency [14]. Similar to Ref. [3] we restrict ourselves by the stepwise behavior with $\epsilon_2 = 1$ as shown in Fig. 1. Then the dielectric cylinder becomes equivalent to a one-dimensional array of dielectric discs with permittivity ϵ_1 .

II. SCATTERING OF PLANE WAVES BY AN ARRAY OF DIELECTRIC DISCS

We consider that the plane wave incidents in the (x, z) plane as shown in Fig. 1. The components of electromagnetic (EM) field for $m \neq 0$ can be written in the cylindrical system of

coordinates via the following equations [3,15]:

$$\begin{aligned} E_\phi &= \frac{i}{m} \frac{\partial \psi_{\text{TE}}}{\partial r}, \quad E_r = \frac{\psi_{\text{TE}}}{r}, \\ H_\phi &= -\frac{i}{k_0 r} \frac{\partial \psi_{\text{TE}}}{\partial z}, \\ H_r &= -\frac{1}{k_0 m} \frac{\partial^2 \psi_{\text{TE}}}{\partial z \partial r}, \\ H_z &= \frac{1}{k_0 m} \left[\frac{\partial^2}{\partial r^2} + \frac{1}{r} \frac{\partial}{\partial r} - \frac{m^2}{r^2} \right] \psi_{\text{TE}}, \end{aligned} \quad (1)$$

and for the TM solution

$$\begin{aligned} H_\phi &= \frac{i\sqrt{\epsilon}}{m} \frac{\partial \psi_{\text{TM}}}{\partial r}, \quad H_r = \frac{\sqrt{\epsilon} \psi_{\text{TM}}}{r}, \\ E_\phi &= \frac{i}{k_0 \epsilon r} \frac{\partial \sqrt{\epsilon} \psi_{\text{TM}}}{\partial z}, \\ E_r &= \frac{1}{k_0 \epsilon m} \frac{\partial \sqrt{\epsilon}}{\partial z} \frac{\partial \psi_{\text{TM}}}{\partial r}, \\ E_z &= -\frac{1}{k_0 \sqrt{\epsilon} m} \left[\frac{\partial^2}{\partial r^2} + \frac{1}{r} \frac{\partial}{\partial r} - \frac{m^2}{r^2} \right] \psi_{\text{TM}}, \end{aligned} \quad (2)$$

where $\sigma = \text{TE, TM}$ and the auxiliary function ψ_σ obeys the equation

$$\left[\frac{\partial^2}{\partial r^2} + \frac{1}{r} \frac{\partial}{\partial r} - \frac{m^2}{r^2} + \frac{\partial^2}{\partial z^2} + U_\sigma(z) \right] \psi_\sigma(z, r) = 0 \quad (3)$$

where

$$U_{\text{TM}}(z) = \epsilon(z) k_0^2 - \frac{3}{4} \left(\frac{\epsilon'(z)}{\epsilon(z)} \right)^2 + \frac{1}{2} \frac{\epsilon''(z)}{\epsilon(z)}, \quad U_{\text{TE}}(z) = \epsilon(z) k_0^2. \quad (4)$$

Because of the axial symmetry and the periodicity of the cylinder we can expand all functions in series of the Bessel functions and Bloch waves [15]

$$\psi_\sigma(r, z) = \sum_{sn} g_{s,\sigma} c_{s\sigma} J_m(\lambda_{s,\sigma} r) e^{i(qn+k_z)z}, \quad (5)$$

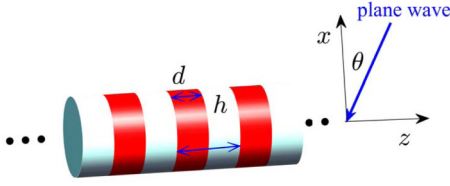


FIG. 1. Infinite circular dielectric cylinder with periodically alternating permittivity ϵ_1 (dark red) and ϵ_2 (light gray).

$$U_\sigma(z) = k_0^2 \sum_n U_n^\sigma e^{iqnz}, \quad q = 2\pi/h, \quad (6)$$

where h is the period of the structure and the eigenvalues λ_σ and eigenvectors \mathbf{c}_σ are found from the eigenvalue problem

$$\widehat{L}^\sigma \mathbf{c}_{s\sigma} = \lambda_{s\sigma}^2 \mathbf{c}_{s\sigma} \quad (7)$$

with the matrix

$$L_{nn'}^\sigma = -(qn + k_z)^2 \delta_{nn'} + k_0^2 U_{n-n'}^\sigma. \quad (8)$$

The equation for the eigenmodes including the BICs with eigenfrequencies above the light line can be presented as $\widehat{H}\vec{\Psi} = 0$. The case of scattering of electromagnetic waves differs from this equation only by the right-hand source term

$$\widehat{H}\vec{\Psi} = \vec{\Phi}^{\text{inc}} \quad (9)$$

where the matrix \widehat{H} was derived in Ref. [3]. The solution $\vec{\Psi} = \begin{pmatrix} \vec{\psi}^{\text{TE}} \\ \vec{\psi}^{\text{TM}} \end{pmatrix}$ and incident wave $\vec{\Phi}^{\text{inc}} = \begin{pmatrix} \vec{\phi}^{\text{TE}} \\ \vec{\phi}^{\text{TM}} \end{pmatrix}$ responses for the incident plane wave in the (x, z) plane are shown in Fig. 1.

Substituting Eq. (5) into Eq. (9) and satisfying the boundary conditions, the following system of algebraic equations for the expansion coefficients $c_{s\sigma}$ can be written [3]:

$$\begin{aligned} im(\widehat{A} - i\widehat{B} - \widehat{T}\widehat{D})\vec{\psi}_{\text{TM}} + k_0 R(\widehat{F} - i\widehat{J}\widehat{P})\vec{\psi}_{\text{TE}} \\ = \delta_{n0} \lambda \frac{mi^m}{\alpha_0} a_{\text{TE}}, \\ k_0 R(\widehat{K} - i\widehat{J}\widehat{P})\vec{\psi}_{\text{TM}} - im\widehat{T}(\widehat{C} - \widehat{D})\vec{\psi}_{\text{TE}} \\ = -\delta_{n0} \lambda \frac{mi^m}{\alpha_0} a_{\text{TM}}, \end{aligned} \quad (10)$$

where $\lambda = k_0 R \alpha_0 [J'_m(\alpha_0 R) - \frac{H'_m(\alpha_0 R)}{H_m(\alpha_0 R)} J_m(\alpha_0 R)]$, $\alpha_n = \sqrt{k_0^2 - (k_z + qn)^2}$, and a_σ are the amplitudes of the incident plane wave with σ th polarization. The right-hand expressions are the result of expansion of the plane wave with the wave vector $\vec{k} = (k_x, 0, k_z)$ in series over cylindrical waves specified by the orbital angular momentum (OAM) m [16].

According to Eq. (5) the s th component of the solutions for vector $\vec{\psi}_\sigma$ is given by

$$(\vec{\psi}_\sigma)_s = g_{s,\sigma} J_m(\lambda_{s,\sigma} R). \quad (11)$$

The elements of matrices in Eq. (10) could be found as

$$\begin{aligned} A_{ns} &= \sum_l b_{n-l}(k_z + ql) c_{sl,\text{TM}}, & B_{ns} &= \sum_l d_{n-l} c_{sl,\text{TM}}, \\ I_{nm} &= \delta_{nm}(k_z + qn), & J_{nm} &= \delta_{nm} \alpha_n \frac{H_m^{(1)}(\alpha_n R)}{H_m^{(1)}(\alpha_n R)}, \end{aligned}$$

$$\begin{aligned} F_{ns} &= \lambda_{s,\text{TE}} c_{sl,\text{TE}} \frac{J'_m(\lambda_{s,\text{TE}} R)}{J_m(\lambda_{s,\text{TE}} R)}, \\ K_{ns} &= \lambda_{s,\text{TE}} \frac{J'_m(\lambda_{s,\text{TE}} R)}{J_m(\lambda_{s,\text{TE}} R)} \sum_l a_{n-l} c_{sl,\text{TE}}, \\ P_{ns} &= \frac{\lambda_{s,\text{TE}}^2}{\alpha_n^2} c_{ns,\text{TE}}, & D_{ns} &= \frac{\lambda_{s,\text{TE}}^2}{\alpha_n^2} \sum_l b_{n-l} c_{sl,\text{TM}}, \end{aligned} \quad (12)$$

where

$$\begin{aligned} \sqrt{\epsilon} &= \sum_n a_n e^{iqnz}, \\ \frac{1}{\sqrt{\epsilon}} &= \sum_n b_n e^{iqnz}, \\ \frac{\epsilon'(z)}{2\epsilon^{3/2}(z)} &= \sum_n d_n e^{iqnz}. \end{aligned} \quad (13)$$

The more simple case with zero OAM $m = 0$ is omitted here. Details can be found in Refs. [3,15].

III. EMERGENCE OF BICS IN SCATTERING

In this section we present the results of numerical solution of Eq. (10) for the scattering of the incident plane wave by a cylinder with a periodically modulated refractive index. To be specific, similarly to Ref. [3] we consider the case of stepwise behavior of the permittivity

$$\epsilon(z) = \epsilon_2 + \frac{1}{2}(\epsilon_1 - \epsilon_2)\{1 - \tanh[\kappa(|z| - 1/2)]\},$$

where the parameter κ controls the sharpness of stepwise behavior. In what follows we take $\kappa = 17$ that is close to the case of a periodical array of dielectric disks shown in Fig. 1. We take the radius of disks $R = R_{0c} - 0.01$ where the BIC with $|m| = 5$ occurs at the point $k_{0c} = 5.14387$, $R_c = 1.8759$, $k_{zc} = 0$ [3]. The pattern of the scattering function in the near zone is shown Fig. 2 where only the azimuthal components E_ϕ and H_ϕ are presented for brevity. One can see that the scattering function in the near zone closely reproduces the BIC mode with $|m| = 5$, symmetry protected with respect to the TE radiation continuum and decoupled from the TM radiation continuum by tuning the radius [3]. The BIC mode profile is shown in the right subplots of Fig. 2. Interestingly it is the electric field that is mostly perturbed under illumination by a circularly polarized wave.

If we take the incident plane wave of pure TE or TM polarization, i.e., $a_{\text{TM}} = 0$ or $a_{\text{TE}} = 0$, the Poynting vector

$$j_\phi = \frac{1}{2} \text{Re}[E_z H_r^* - E_r H_z^*] \quad (14)$$

is odd relative to $y \rightarrow -y$ to give rise to zero Poynting vector after average over ϕ . For the incident TE plane wave we have [17]

$$\begin{aligned} E_z(x, y, z) &= -E_z(x, -y, z), & E_r(x, y, z) &= -E_r(x, -y, z), \\ H_z(x, y, z) &= H_z(x, -y, z), & H_r(x, y, z) &= H_r(x, -y, z). \end{aligned} \quad (15)$$

Therefore we have from Eq. (14) that $j_\phi(x, y, z) = -j_\phi(x, -y, z)$ to give rise to $j_\phi = 0$. We have a similar result

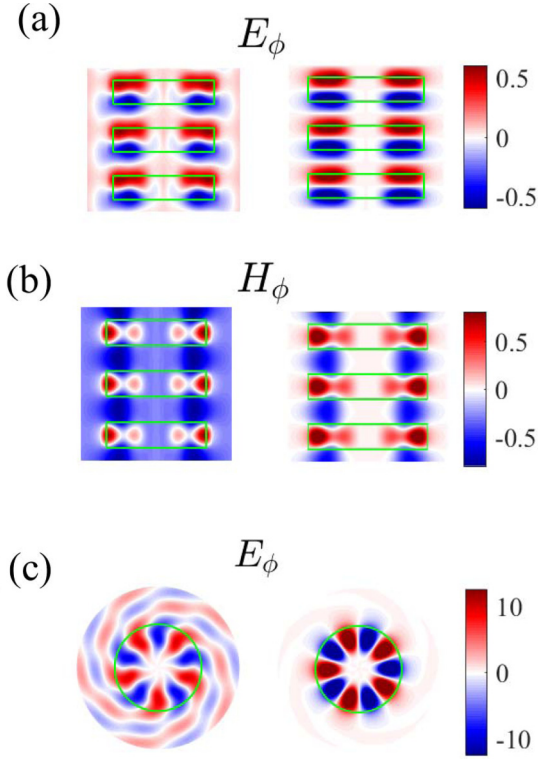


FIG. 2. The azimuthal components of scattered electromagnetic field in the near zone for scattering of an oblique plane wave with circular polarization $a_{\text{TM}} = 1, a_{\text{TE}} = i$ and parameters $k_0 = 5.1523, k_z = 0.03$. (a, b) Scattering field (left) compared to the BIC with $|m| = 5$ with frequency $k_{0c} = 5.14387, R_c = 1.8759, k_{zc} = 0$ in plane (x, z) . (c) In plane $z = 0.5$. The material parameters are $\epsilon_1 = 5, \epsilon_2 = 1, d = 0.5, R = R_c - 0.01$.

for the incident TM plane wave:

$$\begin{aligned} E_z(x, y, z) &= E_z(x, -y, z), & E_r(x, y, z) &= E_r(x, -y, z), \\ H_z(x, y, z) &= -H_z(x, -y, z), & H_r(x, y, z) &= -H_r(x, -y, z). \end{aligned} \quad (16)$$

In general we have

$$\begin{aligned} E_z &= a_{\text{TE}} E_z^{(a)} + a_{\text{TM}} E_z^{(s)}, & H_z &= a_{\text{TE}} H_z^{(s)} + a_{\text{TM}} H_z^{(a)}, \\ E_r &= a_{\text{TE}} E_r^{(a)} + a_{\text{TM}} E_r^{(s)}, & H_r &= a_{\text{TE}} H_r^{(s)} + a_{\text{TM}} H_r^{(a)}, \end{aligned} \quad (17)$$

where superscripts s and a imply even and odd components relative to $y \rightarrow -y$. Substituting these relations into Eq. (14) we obtain that only cross terms of the TE and TM polarization contribute into the Poynting vector averaged over ϕ :

$$\begin{aligned} \langle j_\phi \rangle &= \frac{1}{2} \text{Re} \left\{ a_{\text{TE}} a_{\text{TM}}^* [E_z^{(a)} H_r^{(a)*} - E_r^{(a)} H_z^{(a)*}] \right. \\ &\quad \left. + a_{\text{TE}}^* a_{\text{TM}} [E_z^{(s)} H_r^{(s)*} - E_r^{(s)} H_z^{(s)*}] \right\}, \end{aligned} \quad (18)$$

which is the even part of the Poynting vector relative to $y \rightarrow -y$. Hence in order to excite the Poynting vector circulating around the cylinder we have to apply a plane wave superposed of both polarizations. In particular, it can be the circular polarization for $a_{\text{TE}} = 1, a_{\text{TM}} = i$.

It is worth noting the tremendous role of the angle of incidence given by k_z in the excitation of Poynting currents.

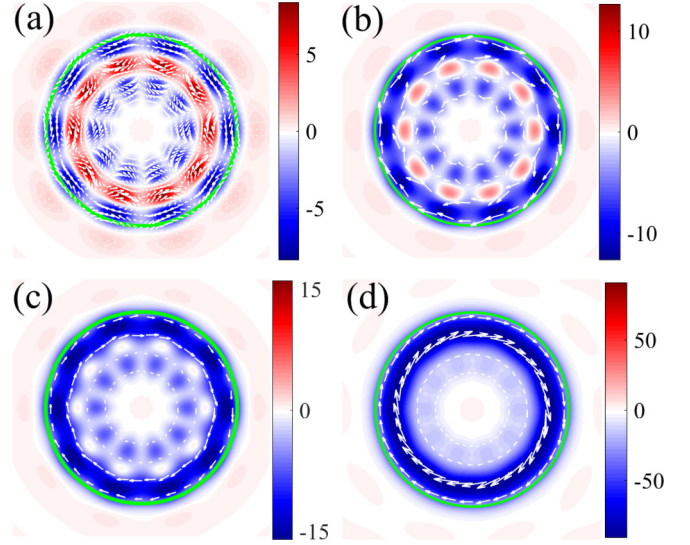


FIG. 3. The azimuthal component of the Poynting vector at $z = 0.25$ for $k_z = 0$ (a), $k_z = 0.000625$ (b), $k_z = 0.00125$ (c), and $k_z = 0.01$ (d) for a circular polarized incident plane wave. Other parameters are given in Fig. 2. These points are shown in Fig. 4 by open circles.

Figure 3 shows that the azimuthal component of the current rearranges after a tiny variation of k_z from zero to $k_z = 10^{-2}$ for the frequency close to the BIC frequency. First, the plane wave with circular polarization excites the Poynting vector even for normal incidence as shown in Fig. 3(a). Due to vicinity to the BIC point with $|m| = 5$ the Poynting vector circulation splits into a cellular structure reflecting the OAM $|m| = 5$. However, the clockwise circulation compensates the anticlockwise circulation, because the net Poynting vector has a relatively small mean value. The smallest deviation of the angle of incidence from zero ($k_z \neq 0$) breaks this symmetry, leading to a dominant contribution of the clockwise circulation as demonstrated in Fig. 3(b). The further deviation of k_z from zero arranges the Poynting vector into almost circular clockwise circulation as shown in Figs. 3(c) and 3(d). The quantitative results for $\langle j_\phi \rangle$ are presented in Fig. 4, which shows the maximal and minimal Poynting vector in the plane (x, z) . One can see from this figure that maximal and minimal values of the Poynting vector show resonant behavior as dependent on the frequency and the angle of incidence. Moreover these extremal values are defined by the sign of k_z to give rise to the vortical Poynting vector as illustrated in Fig. 3. Figure 5 shows the dependence of the mean Poynting vector on the rotation of

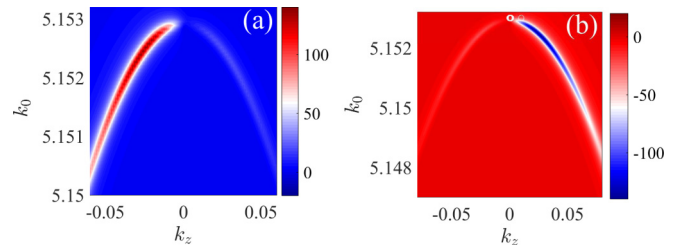


FIG. 4. Maximal (a) and minimal (b) values of the azimuthal component of the Poynting vector vs k_z and frequency k_0 at the section (x, z) for $R = R_c - 0.01$. Other parameters are given in Fig. 2.

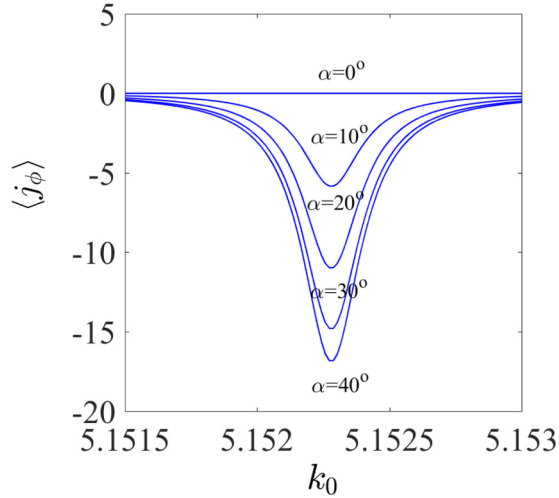


FIG. 5. Evolution of the energy flux with rotation of the polarization of the plane wave with $k_z = 0.01$ vs frequency for $R = R_c - 0.01$.

polarization given by $a_{TE} = \sin \alpha, a_{TM} = \cos \alpha$. Both Figs. 4 and 5 demonstrate that the energy flux follows the polarization: in the interval $\alpha = (0, \pi/4)$ the current is increasing and then in the interval $\alpha = (\pi/4, \pi/2)$ it is decreasing. In the next interval the flux shows the same behavior with a change of the sign.

The incident plane wave with the polarization σ excites, respectively, the quasi BIC with the same OAM and polarization for the parameters of the cylinder and the frequency close to the BIC point. In fact we consider the scattering of a plane wave which can be expanded over the cylindrical waves given by Eqs. (1) and (2). Then the plane wave with circular polarization incident almost normally to the cylinder is capable to excite the BICs with OAM performing a transfer of spin angular momentum into the orbital angular momentum of the BICs as it was shown in the array of dielectric spheres [18]. Moreover, the spin angular momentum can transfer to the orbital angular momentum of the propagating Bloch wave [19] with extremely high efficiency if the frequency of the incident wave is close to the frequency of this BIC. Similar phenomena take place for the stack of dielectric discs, however the OAM of the excited scattering function can be higher compared to the array of spheres because of excitation of appropriate BICs shown in Figs. 2 and 3.

Figure 6 illustrates the behavior of the cross section. There are two important aspects of dependence on the frequency, polarization and the angle of incidence. The first aspect is the narrowing of resonant width and collapse of the Fano resonance that is typical on approach to the BIC point [5]. The second aspect is tuning Fano resonance with no variation of material parameters [13]. Figure 6 demonstrates a substantial change of the Fano resonance profile with a sweep of the angle of incidence.

IV. SUMMARY

Under illumination by plane wave with frequency close to the BIC point the scattering solution can be very similar to the BIC mode. This phenomenon was previously described

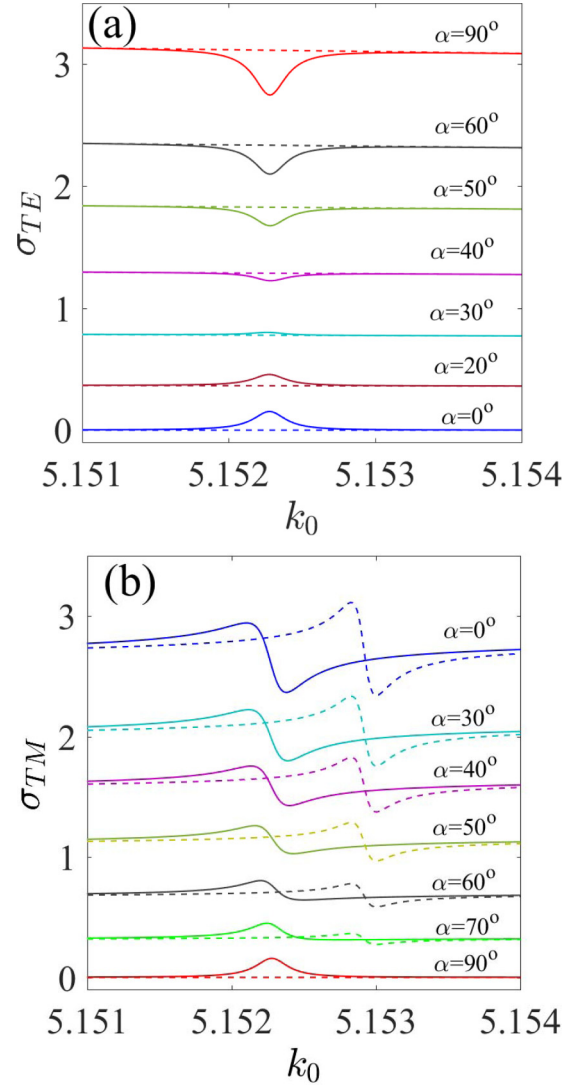


FIG. 6. Evolution of the cross section for scattering into the TE (a) and TM (b) channels with rotation of the polarization of the plane wave at normal incidence ($k_z = 0$ dashed lines) and at near normal incidence $k_z = 0.03$ (solid lines). The polarization of the incident wave is given by angle α via $a_{TE} = \cos \alpha, a_{TM} = \sin \alpha$.

in the framework of the two-level Fano-Anderson model [5]. In application to the stack of dielectric disks this result is well illustrated by Fig. 2. However, there are a few important specific details related to vectorial BIC solutions, rotational symmetry of the stack and geometry of scattering. The most striking result is related to excitation of Bloch BICs running along the stack above the light line. This effect turns out to be very sensitive to the angle of incidence. Thus, that system brings in a new generation of fibers with extremely high Q factor provided that the parameters of the trapped propagating mode are close to the BIC point [19–24].

The next interesting result is that scattering of an oblique plane wave with mixed polarization allows us to vary the profile of Fano resonance only by rotation of the polarization of the wave not addressing tuning of material parameters [13]. This effect becomes especially sensitive to variation of external parameters in the vicinity of the BIC frequency [14]. Indeed,

the change of the angle of incidence gives rise to even more cardinal rearrangement of the cross sections. In the vicinity of the BIC frequency the em field is strongly enhanced. The next feature is related to the OAM of BICs. An application of the plane wave with TE and TM polarizations mixed excites the giant Poynting vector circulating in directions defined by the angle of incidence or the polarization.

ACKNOWLEDGMENTS

We acknowledge discussions with A. A. Bogdanov and D. N. Maksimov. This paper was partially supported by Ministry of Education and Science of Russian Federation (State Contract No. 3.1845.2017) and Russian Foundation for Basic Research Grant No. 16-02-00314.

-
- [1] L. Rayleigh, The dispersal of light by a dielectric cylinder, *Philos. Mag.* **36**, 365 (1918).
- [2] J. R. Wait, Scattering of a plane wave from a circular dielectric cylinder at oblique incidence, *Can. J. Phys.* **33**, 189 (1955).
- [3] E. N. Bulgakov and A. F. Sadreev, Bound states in the continuum with high orbital angular momentum in a dielectric rod with periodically modulated permittivity, *Phys. Rev. A* **96**, 013841 (2017).
- [4] X. Gao, C. W. Hsu, B. Zhen, M. Soljacic, and H. Chen, Bound states in the continuum in low-contrast fiber Bragg gratings, [arXiv:1707.01247](https://arxiv.org/abs/1707.01247) (2017).
- [5] A. F. Sadreev, E. N. Bulgakov, and I. Rotter, Bound states in the continuum in open quantum billiards with a variable shape, *Phys. Rev. B* **73**, 235342 (2006).
- [6] M. Zhang and X. Zhang, Ultrasensitive optical absorption in graphene based on bound states in the continuum, *Sci. Rep.* **5**, 8266 (2015).
- [7] V. Mocella and S. Romano, Giant field enhancement in photonic resonant lattices, *Phys. Rev. B* **92**, 155117 (2015).
- [8] J. W. Yoon, S. H. Song, and R. Magnusson, Critical field enhancement of asymptotic optical bound states in the continuum, *Sci. Rep.* **5**, 18301 (2016).
- [9] E. N. Bulgakov and D. N. Maksimov, Light enhancement by quasi-bound states in the continuum in dielectric arrays, *Opt. Express* **25**, 14134 (2017).
- [10] C. S. Kim, A. M. Satanin, Y. S. Joe, and R. M. Cosby, Resonant tunneling in a quantum waveguide: Effect of a finite-size attractive impurity, *Phys. Rev. B* **60**, 10962 (1999).
- [11] S. Venakides and S. P. Shipman, Resonance and bound states in photonic crystal slabs, *SIAM J. Appl. Math.* **64**, 322 (2003).
- [12] M. L. Ladrón de Guevara, F. Claro, and P. A. Orellana, Ghost Fano resonance in a double quantum dot molecule attached to leads, *Phys. Rev. B* **67**, 195335 (2003).
- [13] F. Xiao, W. Zhu, M. Premaratne, and J. Zhao, Controlling Fano resonance of ring/crescent-ring plasmonic nanostructure with Bessel beam, *Opt. Express* **22**, 2132 (2014).
- [14] M. V. Rybin, K. L. Koshelev, Z. F. Sadrieva, K. B. Samusev, A. A. Bogdanov, M. F. Limonov, and Yu. S. Kivshar, High-Q Supercavity Modes in Subwavelength Dielectric Resonators, *Phys. Rev. Lett.* **119**, 243901 (2017).
- [15] J. Li and N. Engheta, Subwavelength plasmonic cavity resonator on a nanowire with periodic permittivity variation, *Phys. Rev. B* **74**, 115125 (2006).
- [16] D. Maystre, S. Enoch, and G. Tayeb, Scattering matrix method applied to photonic crystals, in *Electromagnetic Theory and Applications for Photonic Crystals*, edited by K. Yasumoto (Taylor & Francis, London, 2006).
- [17] D. Marcuse, *Light Transmission Optics* (Van Nostrand, Princeton, 1982).
- [18] E. N. Bulgakov and A. F. Sadreev, Transfer of spin angular momentum of an incident wave into orbital angular momentum of the bound states in the continuum in an array of dielectric spheres, *Phys. Rev. A* **94**, 033856 (2016).
- [19] E. N. Bulgakov and A. F. Sadreev, Propagating Bloch bound states with orbital angular momentum above the light line in the array of dielectric spheres, *J. Opt. Soc. Am. A* **34**, 949 (2017).
- [20] C. W. Hsu, B. Zhen, S.-L. Chua, S. G. Johnson, J. D. Joannopoulos, and M. Soljačić, Bloch surface eigen states with in the radiation continuum, *Light: Sci. Appl.* **2**, e84 (2013).
- [21] E. N. Bulgakov and D. N. Maksimov, Light guiding above the light line in arrays of dielectric nanospheres, *Opt. Lett.* **41**, 3888 (2016).
- [22] E. N. Bulgakov and D. N. Maksimov, Bound states in the continuum and polarization singularities in periodic arrays of dielectric rods, *Phys. Rev. A* **96**, 063833 (2017).
- [23] L. Yuan and Y. Y. Lu, Propagating Bloch modes above the lightline on a periodic array of cylinders, *J. Phys. B* **50**, 05LT01 (2017).
- [24] C.-L. Zou, J.-M. Cui, F.-W. Sun, X. Xiong, X.-B. Zou, Z.-F. Han, and G.-C. Guo, Guiding light through optical bound states in the continuum for ultrahigh-Q microresonators, *Laser Photon. Rev.* **9**, 114 (2015).